Project no. GOCE-CT-2003-505539

Project acronym: ENSEMBLES

Project title: ENSEMBLE-based Predictions of Climate Changes and their Impacts

Instrument: Integrated Project

Thematic Priority: Global Change and Ecosystems

Deliverable D6.2 First phase impact models to predict damage to human activities, the environment and tropical annual crops from climate extremes, e.g. wind storm, drought, flood, and heat stress

Due date of deliverable: month 18
Actual submission date: first draft: month 21, this revision: month 25

Start date of project: 1 September 2004 Duration: 60 Months

Lead Partner: UEA: University of East Anglia, Norwich, UK
Contributing Partners: NAO: National Observatory of Athens, Greece
UREADMM: CGAM, University of Reading, UK
FUB: Free University of Berlin, Germany

Revision [2]

Project co-funded by the European Commission within the Sixth Framework Programme (2002-2006)		
Dissemination Level		
PU	Public	x
PP	Restricted to other programme participants (including the Commission Services)	
RE	Restricted to a group specified by the consortium (including the Commission Services)	
CO	Confidential, only for members of the Consortium (including the Commission Services)	

Introduction

This report fulfils the requirements of ENSEMBLES Deliverable D6.2: First phase impact models to predict damage to human activities, the environment and tropical annual crops from climate extremes, e.g. wind storm, drought, flood, and heat stress. The methodology extends the work of the Framework V projects MICE and PRUDENCE to include more explicit models of the impacts of climate extremes on human activity. As ENSEMBLES model data comes on stream, these advances will be augmented by much more sophisticated assessment of the uncertainty in projected impacts than was possible in the earlier studies. Moreover, for the first time, the responses to climate extremes will be assessed at high spatial resolution for a continuous period to 2100. As well as enabling the study of the response of human systems to climate extremes for the crucial mid-century period, these data will allow extended study of return levels and very detailed and reliable estimates of the probability of achieving particular critical impact thresholds. The report contains four contributions covering various aspects of the impact models specified in the Deliverable.

Summary of contents

1) Effects of climate change on Health, Heat Stress, Wind Storm, Flood, and Return Levels (UEA) (pages 4-27)

This report covers the indicated topics over the whole of Europe. It presents the state of the impact models at month 18. All the example analyses are presented using data from the fairly coarse spatial resolution GCM HadCM3. This is chosen because it provides data with continuous time series, similar to the data that will come from the Regional Climate Models of ENSEMBLES. Therefore, although the results are not genuinely representative of extremes because of spatial smoothing, the methods will work virtually unchanged with the ENSEMBLES RCM data. Of particular importance is the section on return levels. Although not stated, a corollary of robust estimation of return levels is estimates of the probability of particular thresholds crucial for impacts analysis. For example, a grid-point value described as a 1 in 100 year event, has a 1% chance of occurring in any year. This property of the Generalised Extreme Value Distribution will be further exploited in subsequent studies.

2) GLAM tropical crop model (UREADMM) (pages 28-30)

The GLAM model studies of tropical crops provide an important extension to the general ENSEMBLES domain of Europe. These highly detailed experiments examine the crucial influence of short term temperature extremes on the productivity of groundnut, wheat, and rice.

3) A Heat Index for Heat Stress studies (NOA) (pages 31-32)

This model formulates a heat index using detailed heat stress case study data from Athens. Hospital admissions data are incorporated.

4) A Storm Damage Regression Model (FUB) (page 33)

This section summarises the status of a Storm Damage Regression Model for property. This is highly relevant to stakeholders, particularly in the insurance and construction industries.

Next stages

All the impact models described here are under continuous development in terms of the climate extremes considered and relevance to stakeholders. Recent improvements include the incorporation of population density data into some models and the addition of livestock models. The population data will be combined with models of river flooding to give more accurate estimates of flood risk. A high resolution terrain database may also be usefully incorporated into the flood model.

A report on preliminary projections of the impacts of climate extremes will be produced by month 30 under D6.8.

Contribution to ENSEMBLES Deliverable D6.2

Report from UEA: Impact models for Health, Heat Stress, Wind Storm, Flood, and Return Levels

Tom Holt, University of East Anglia, Norwich, UK

Introduction

The ENSEMBLES First Phase Models of damage to human activities under climate change use data from the Hadley Centre global climate model (GCM) HadCM3 to develop the software. Although this model has relatively coarse spatial resolution when compared with the Regional Climate Models (RCMs) being run in ENSEMBLES, it has the advantage of producing continuous time series. RCMs prior to ENSEMBLES typically provide data for two thirty year periods – 1961-90 and 2070-99. To ensure that the logistics of running the models will work with the high resolution RCM data, the HadCM3 climate indices are interpolated onto a 0.5° x 0.5° latitude/longitude grid prior to analysis and presentation.

This part of the impact model development phase is dedicated to producing models examining likely climate-induced changes in the following sectors:

- human health
- heat stress
- wind storm
- return levels

Although there is some overlap between the sectors, for example heat stress has obvious implications for human health, the above divisions focus the research making it more relevant to the interests of particular stakeholders. At the same time, we are able to consider factors relevant to one sector but not to another. For example, although wind storm can affect health, it can also involve costs to the property insurance industry for reasons not necessarily of interest to health workers.

The models presented here will be used with little modification to produce results from Phase 2 of ENSEMBLES using high resolution RCM data. However, it is important to note that the results contained in this report are demonstration only and can be expected to change under Phase 2 of ENSEMBLES. The main purpose of this stage of the research is to test the models and to provide a basis for consultation with stakeholders on the usefulness of the approaches taken. It is likely that further refinements to the models will be necessary following such consultation.

Data

The analysis are performed on 32 climate indices derived from HadCM3 daily variables. The indices over the period 1860-2099 are:

- Derived from daily maximum temperature (tmax)
  - 7-day running mean tmax
  - 95th percentile (over 1961-99) of July tmax
  - 99th percentile (over 1961-99) of July tmax
  - annual number of exceedences of the 95th percentile (over 1961-99) of July tmax (here, exceedences means temperatures higher than the percentile)
  - annual number of exceedences of the 99th percentile (over 1961-99) of July tmax
  - number of times per year tmax exceeded 25°C
- Derived from daily minimum temperature (tmin)
  - 5th percentile (over 1961-99) of January tmin
  - annual number of exceedences of the 5th percentile (over 1961-99) of January tmin (here, exceedences means temperatures lower than the percentile)
  - number of times per year tmin was below 0°C
- Derived from daily mean temperature (tmean)
  - 83rd percentile (over 1961-99) of tmean
  - 95th percentile (over 1961-99) of tmean
  - annual number of exceedences of the 95th percentile (over 1961-99) of tmean (here, exceedences means temperatures higher than the percentile)
  - annual number of exceedences of the 83rd percentile (over 1961-99) of tmean (here, exceedences means temperatures lower than the percentile)
- Derived from daily total rainfall (ppt)
  - 95th percentile (over 1961-99) of ppt
  - annual number of exceedences of the 95th percentile (over 1961-99) of ppt
  - annual maximum length of dry spell
  - annual maximum running 3-day total rainfall
- Derived from daily mean wind speed (wind)
  - 95th percentile (over 1961-99) of wind
  - annual number of exceedences of the 95th percentile (over 1961-99) of wind
  - annual number of days when wind was below 2 m/s
  - the days (1860-2099) when wind was below 2 m/s
- Derived from daily maximum wind speed (wmax)
  - 95th percentile (over 1961-99) of wmax
  - annual number of exceedences of the 95th percentile (over 1961-99) of wmax
  - annual number of days when wmax was above 20 m/s
  - annual number of days when wmax was above 33 m/s
  - annual number of days when wmax was above 45 m/s
  - annual number of days with gales
  - annual number of days with strong gales
  - annual number of days with storms
  - annual number of days with violent storms
  - annual number of days with hurricanes
- Derived from joint distributions of tmax and wind, and tmin and wind
  - annual number of days with tmax higher than 25°C and wind lower than 2 m/s
  - annual number of days with tmin lower than 0°C and wind lower than 2 m/s/

Human Health

Introduction

Climate can affect health directly, as in heat waves, or indirectly through changes in geophysical, ecological and socio-economic systems which themselves affect human health. Indirect effects can be highly complex, possibly requiring the study of several interacting systems to demonstrate climate causation.

In addition to radiatively-forced climate change, climate at local scales can be influenced by other drivers such as land use change and urbanization. Since most of the global population lives in areas which are undergoing some form of landscape transformation, such factors may be important for human health issues.

Moreover, climate change does not occur in isolation, but against a background of possibly more important, in terms of human activity, changes in factors such as biodiversity, employment, and economic growth or decline.

The above summary is taken from an unpublished review (Holt and Betts, 2006) which summarises the factors affecting climate change and health, and itemises the ideal data requirements for examining those factors. It is not possible in ENSEMBLES to account for all the complex interactions and feedbacks implied above. This is particularly the case for a pan-European study where there are likely to be large variations in the quality and availability of scientific, social, and economic data. Here we focus on climate-health relationships which are likely to lend themselves to successful analysis using the model data provided by ENSEMBLES.

There are two approaches to giving the research a European context:

1. Use health models and data from each country. The main problem with this approach is that the models and quality and availability of data will vary hugely from country to country, making the presentation of homogeneous results impossible.
2. Use models and data from a single country and try to adapt the results to other countries. The main drawback in this approach is that models for one country will not necessarily be applicable in another. It is also important to consider that there may be health problems in one region that do not apply in another.

Here, we take the second approach, using models based on the UK as analogues for the rest of Europe. The main advantage of this approach is that results are not country-specific and can be presented as spatially continuous over the whole region. In many cases, the models require no modification to apply in different countries. Where this does not apply, for example the response to high temperatures depends on the conditions people are used to, some form of adjustment to the model is necessary.

Pollution episodes

The ambient climatic conditions for pollution episodes are when wind speed is below 2 m/s for at least one hour in a day and, at the same time either, maximum daily temperature higher than 25°C for summer pollution episodes, or minimum daily temperature below 0°C for winter pollution episodes. Lacking hourly wind speed data, we use as our wind speed criterion mean daily wind speed below 2 m/s. Thus, it will normally indicate less windy conditions than the standard low wind speed criterion. This could give more pollution episodes than the wind speed threshold in the original model. However, this does not matter at

this stage since there is no point in attempting a correction until the model is based on ENSEMBLES RCM data. Moreover, in considering future climate change, it is the relative change in pollution episodes between now and the future that is of interest. This is not likely to be unduly influenced by the level of wind speed threshold. It is assumed that the same model thresholds apply for all of Europe without any regional adjustment.

Winter pollution episodes

Figure 1 shows time series of the annual frequency of climate conditions appropriate for winter pollution episodes over different parts of Europe for the period 1860-2099. Note that in this, and similar plots, the raw time series are shown by the dashed red line and the main features of the series are highlighted by smoothing using the unbiased Hodrick-Prescott filter. Other things being equal, the indications are that the frequency of winter pollution episodes over the whole of Europe will by considerably reduced by the end of the century. Interestingly, this appears to be part of a long-term trend rather than the effect of global warming. Most likely the trend is due to winter warming associated with the end of the Little Ice Age early in the 19th century. After about 2050 the charts for southeastern England and central Spain, particularly, do indicate a response to global warming augmenting the effect of the long-term trend. The climate change signal over Greece appears to be particularly weak.

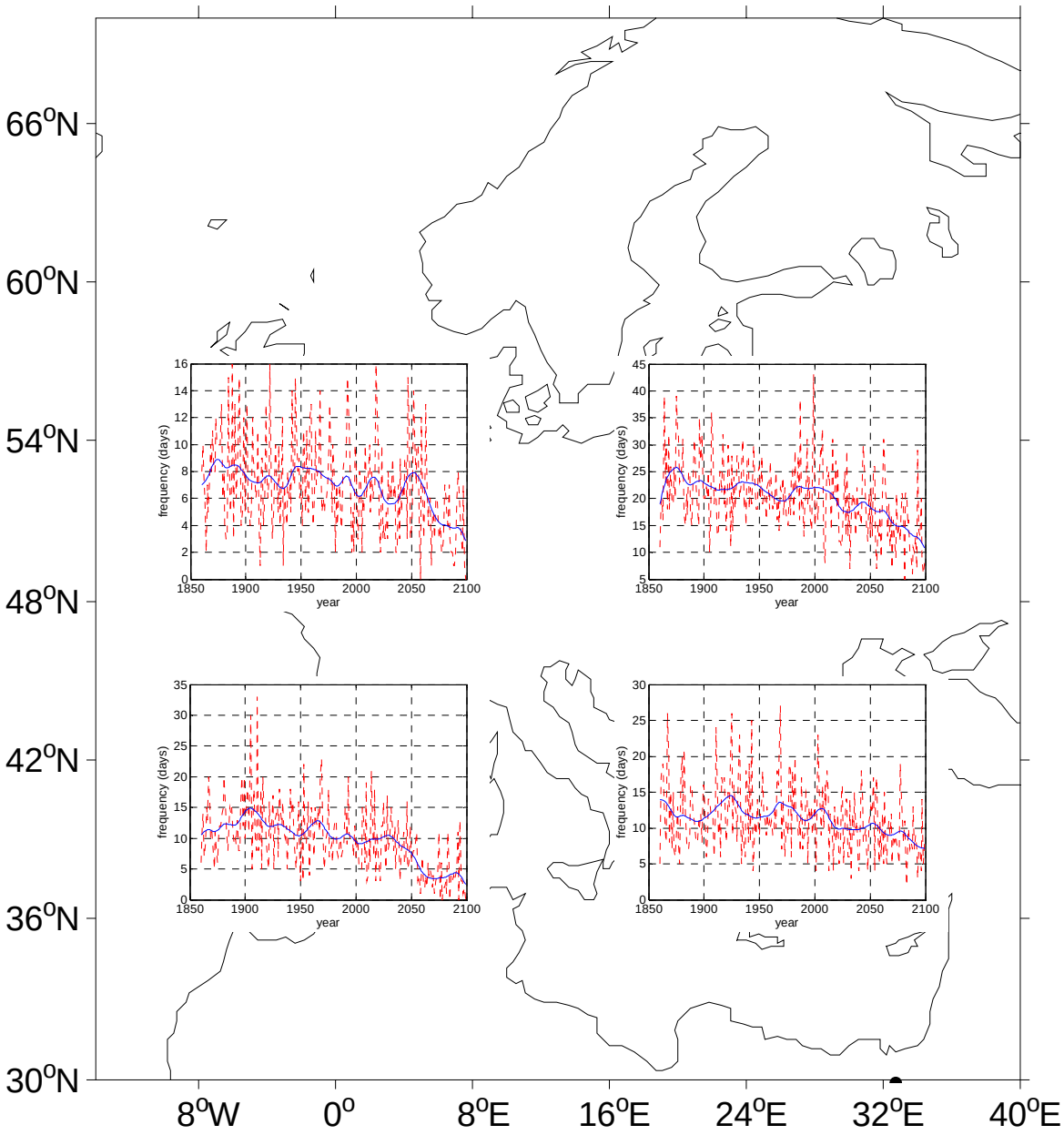

Figure 1 The annual frequency of conditions associated with winter pollution episodes

Summer pollution episodes

Figure 2 shows time series of the annual frequency of climate conditions appropriate for summer pollution episodes over different parts of Europe for the period 1860-2099. As might be expected, summer pollution episodes can be expected to become more frequent under global warming. This time, there is no indication of long-term trend, with the global warming signal manifesting itself about 2000. Again, the global warming signal is weak over Greece.

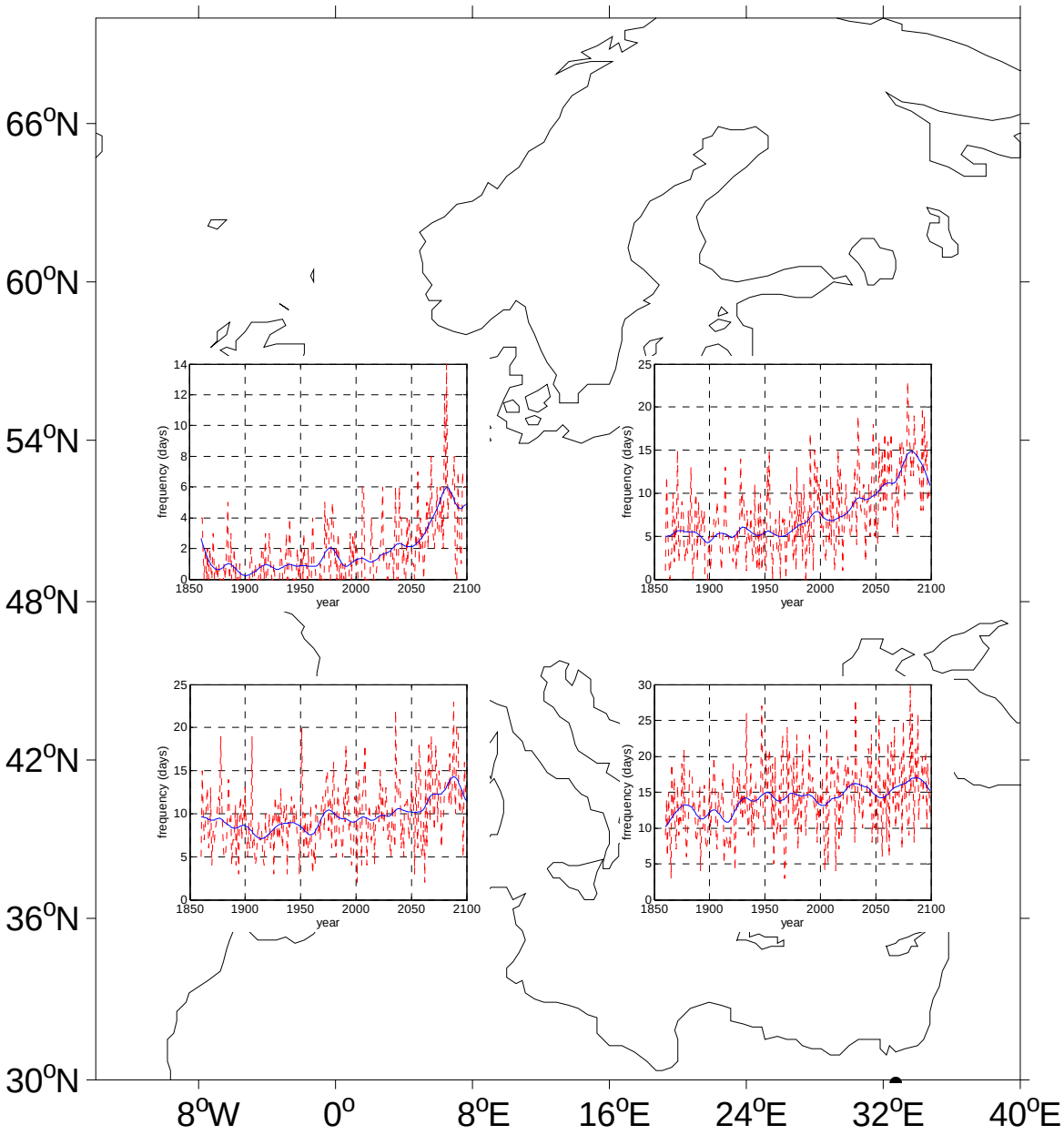

Figure 2 The annual frequency of conditions associated with summer pollution episodes

Conclusions

Since this is a demonstration analysis, there is little purpose in entering a detailed discussion on the meaning of the analysis of pollution episodes. It should be noted, however, that although the projected increase in summer pollution episodes will be offset, to an extent, by the expected reduced frequency of winter episodes, the main factor mitigating the apparent increase in summer pollution will be the concurrent influence of emissions control policy. The likely net effect of the projections shown in Figures 1 and 2, is minimal assuming adherence to current thinking on controlling traffic pollution.

Minimum mortality band for temperature

A minimum mortality band for the UK uses thresholds from temperatures over Central England. Below 15.6°C and above 18.6°C temperature-related deaths begin to increase. To examine this over Europe, we express the band as percentiles, rounding to avoid spurious precision. As shown in Figure 3, the above bands equate to the 83rd and 95th percentiles of daily mean temperature from HadCM3 for the grid point 52.5°N and 0°E over the period 1961-1990. Note that the actual values of these percentiles are 15.58°C and 18.95°C, respectively.

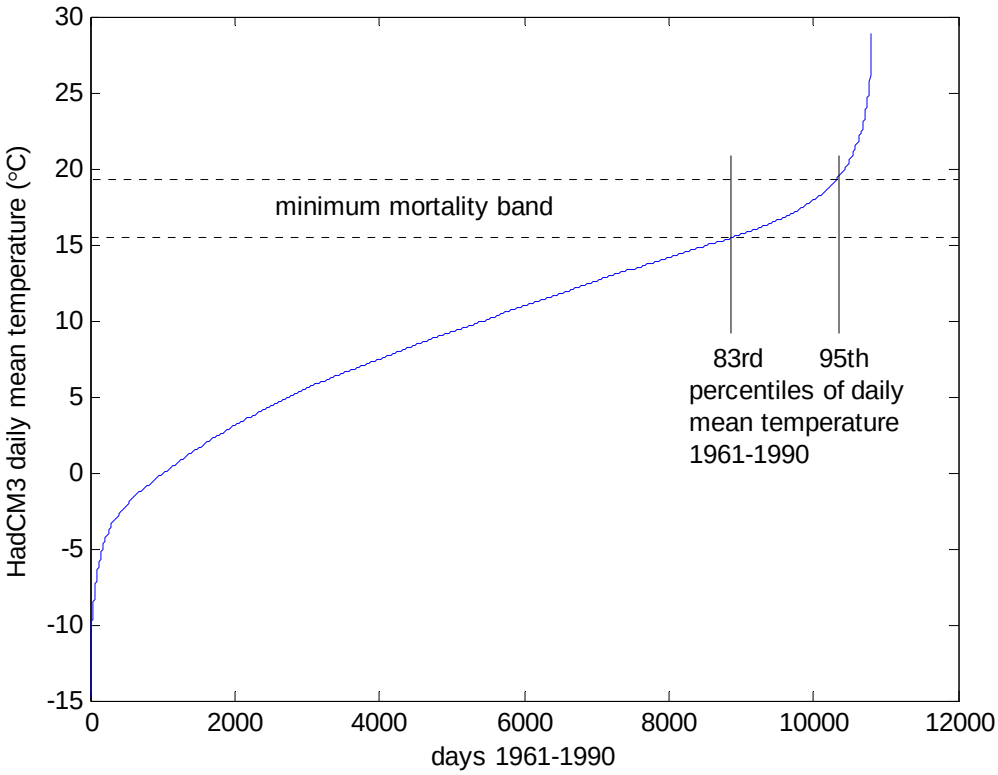

Figure 3 Minimum mortality band from HadCM3 mean daily temperatures (1961-90)

The mortality response to temperature roughly follows the form of the distribution of temperatures in Figure 3. That is, heat-related mortality becomes more severe with relatively small increases in temperature. Cold-related mortality increases much more gradually as temperatures fall until the threshold passes 0°C. We assume that a similar model applies to other European countries and estimate the equivalent percentiles for different HadCM3 grid points.

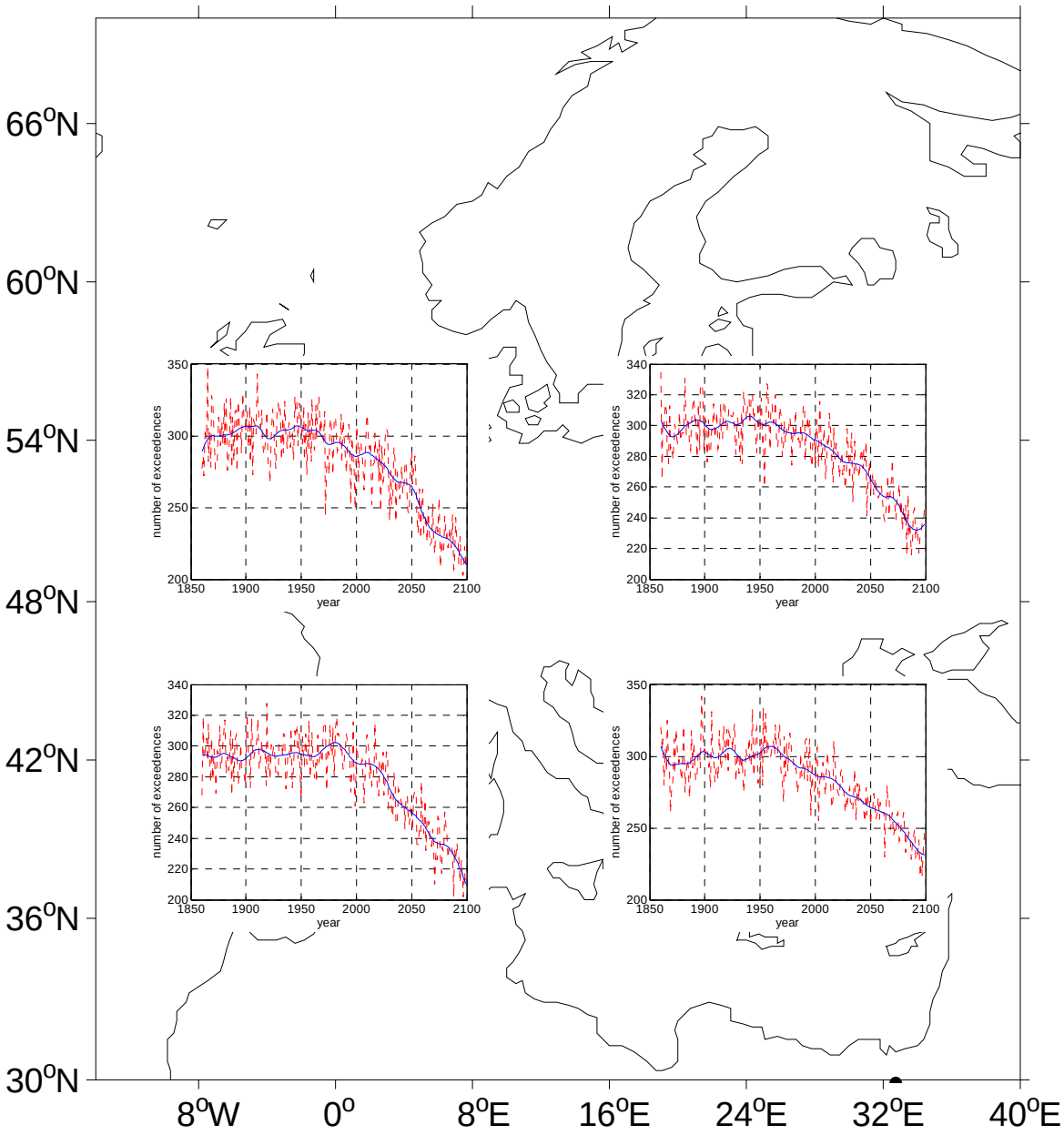

Figure 4 Annual number of times tmean was below the 83rd percentile (1961-90) over the period 1860-2099 for different locations in Europe

Figure 4 shows the number of times each year that tmean was below the 1961-90 83rd percentile over the period 1860-2099. In each case there is a pronounced response to global warming after about 2000, with a marked decrease in occurrences of colder weather compared with the historical period.

Figure 5 shows the number of times each year that tmean was above the 1961-90 95th percentile over the period 1860-2099. Here, the response to global warming also occurs about 2000 but is manifested as a marked increase in the frequency of warmer days compared with the historical period.

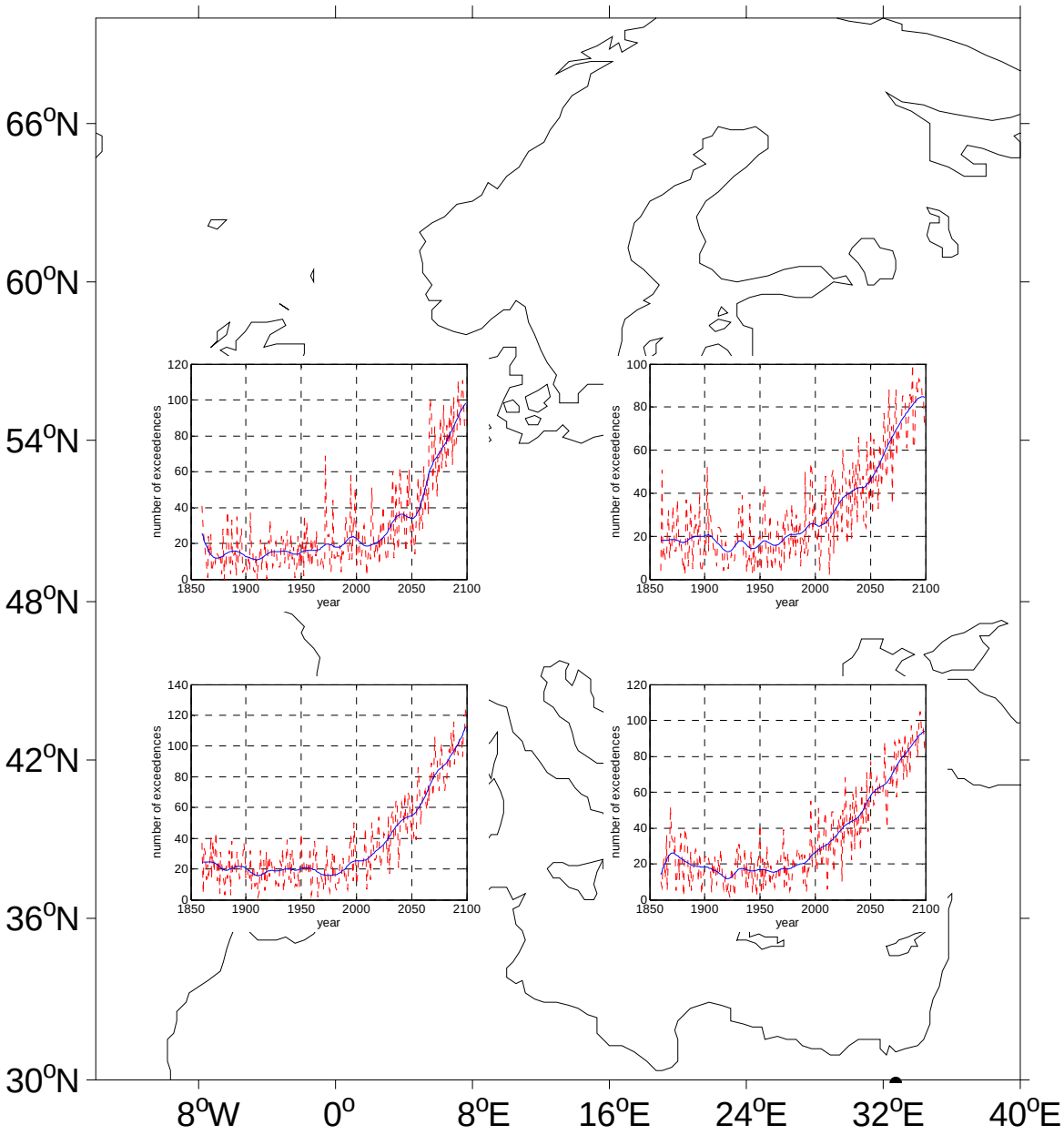

Figure 5 Annual number of times tmean was above the 95th percentile (1961-90) over the period 1860-2099 for different locations in Europe

Conclusions

The exceedences of the lower and upper bounds of the minimum mortality bound, shown in Figures 4 and 5 respectively, indicate that under global warming winter mortality will decline and summer mortality will increase, with the consequences being more or less evenly distributed over Europe. Since it is easier and cheaper to mitigate hot weather mortality than cold weather mortality, it is reasonable to assume that in this context the net effect of global warming will be benign.

Storms

Storms affect health directly by causing death or accidents. Key threshold wind speeds can be related to classes of response:

- Wind gust above 20 m/s – threshold for wind-related road traffic accidents
- Wind gust above 33 m/s – threshold for injuries due to wind-borne building debris and being blown over
- Wind gust above 45 m/s – threshold for injuries due to falling trees and displaced mobile homes

Unfortunately, the spatial resolution of the HadCM3 data is so coarse that most wind speeds above 20 m/s are smoothed out. This is because the atmospheric process resolution of data is half the spatial resolution. Therefore, the pressure gradient for calculating wind is over distances of the order of 1000 km, far too coarse to resolve mid-latitude storm systems. The software is written to examine the above thresholds, but the analysis awaits the high resolution ENSEMBLES RCM data. A further complication is that most models do not provide wind gust, rather they yield maximum daily wind speed – wmax. In the case of HadCM3, this is the highest instantaneous value of wind speed in a day on a single 30 minute timestep. This time interval is too coarse to give a reliable estimate of gust speed.

To give some idea of the behaviour of the wind field over Europe, Figure 6 shows the 95th percentile of wmax over the period 1961-90. According to these data, the highest wind speeds are found over the oceans, coastal regions, and Russia. For most of Europe, therefore, health risks from wind appear not to be a serious problem.

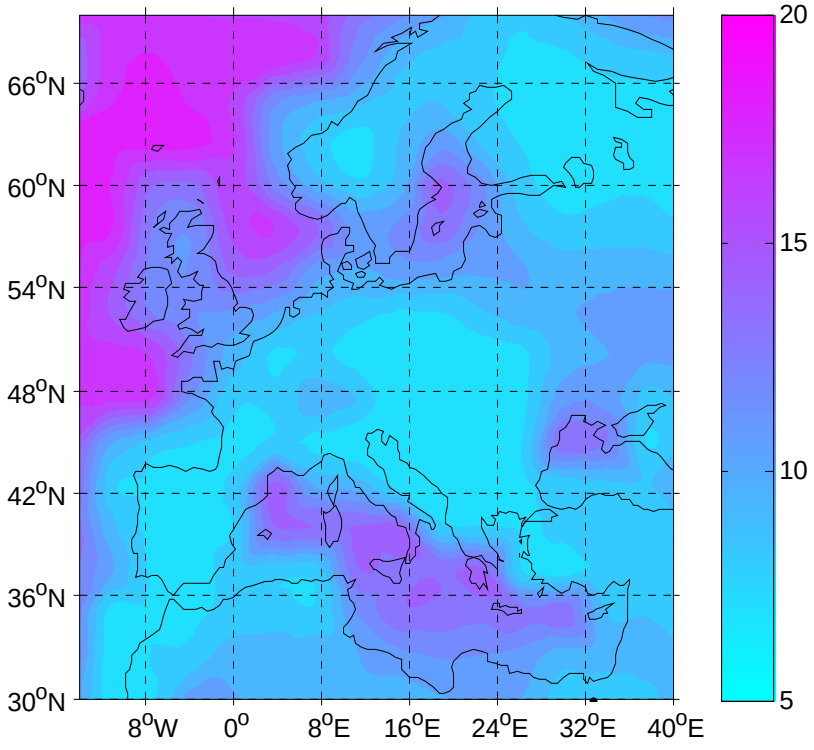

Figure 6 95th percentile (1961-90) of daily maximum wind speed (m/s

Turning now to the time series features of wmax, Figure 7 shows the annual number of exceedences of the 95th percentile (1961-90) for the period 1860-2099. There is some indication that future daily maximum wind speeds may be more variable and slightly more

frequent than at present, but not a particularly strong indication of any response to global warming. On the basis of these data, it is reasonable to assume that wind-related injury and mortality will be unaffected by climate change over Europe.

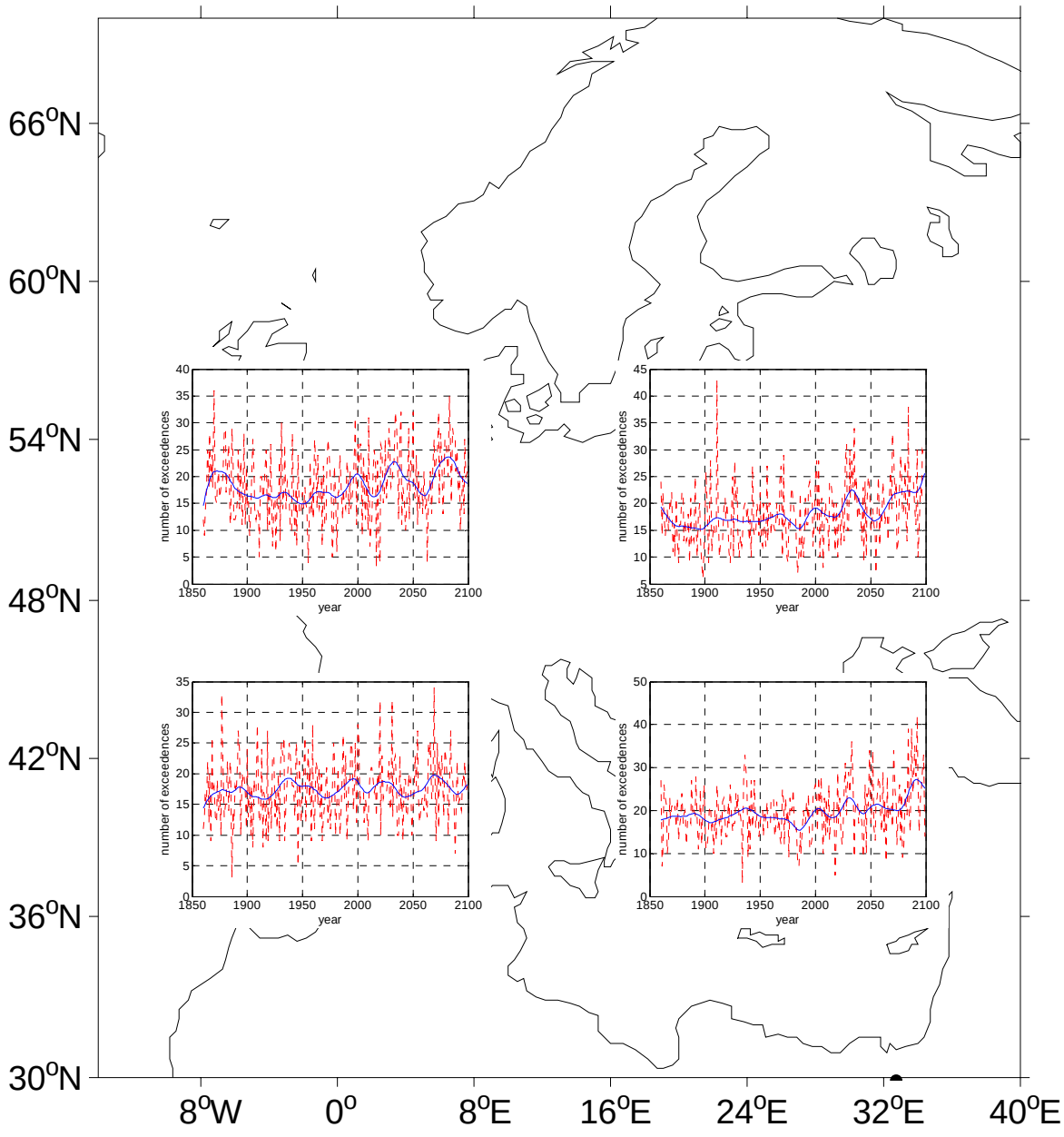

Figure 7 Exceedences of the 95th percentile (1961-90) of daily maximum wind speed (m/s

Rainfall

The evidence from recent events is that disease related to water shortages and flooding, consequences of too little and too much rainfall, respectively, is not a major factor in highly developed regions such as Europe. Also, although flooding is associated with direct health effects in terms of injury and death, particularly in very severe events such as occurred in southern Poland in 1997, at least equally important is the stress-related illness the follows when people are trying to reconstruct their lives. In the weeks following the Polish event, for example, there were several suicides directly associated with such things as the trauma of

sudden homelessness. It is important to note that here we are not dealing with flooding associated with storm surges at the coast, rather flooding associated with high riverflow following heavy rainfall.

Clearly, the impact of high or low rainfall is related to what people expect. Figure 8 shows the modelled 95th percentile of daily total rainfall (1961-90) for Europe. Rainfall is one of the most difficult parameters to model successfully, particularly with a low resolution model which cannot represent complex topography in a realistic way. Therefore, the very high rainfall associated with the Alps, northern Spain, southern Norway, and over Greece and Turkey, should be treated with suspicion. Fortunately, high resolution RCMs tend to perform better than GCMs with regard to rainfall, so the results from these models in the later stages of ENSEMBLES should be much improved.

The time series of exceedences of the 95 perecentile of 1961-90 rainfall (Figure 9) indicate that northern Europe is projected to experience slightly more heavy rainfall events towards the end of the century, Greece no change, and Spain is likely to experience fewer heavy rainfall events. These changes are unlikely to have any impact on health.

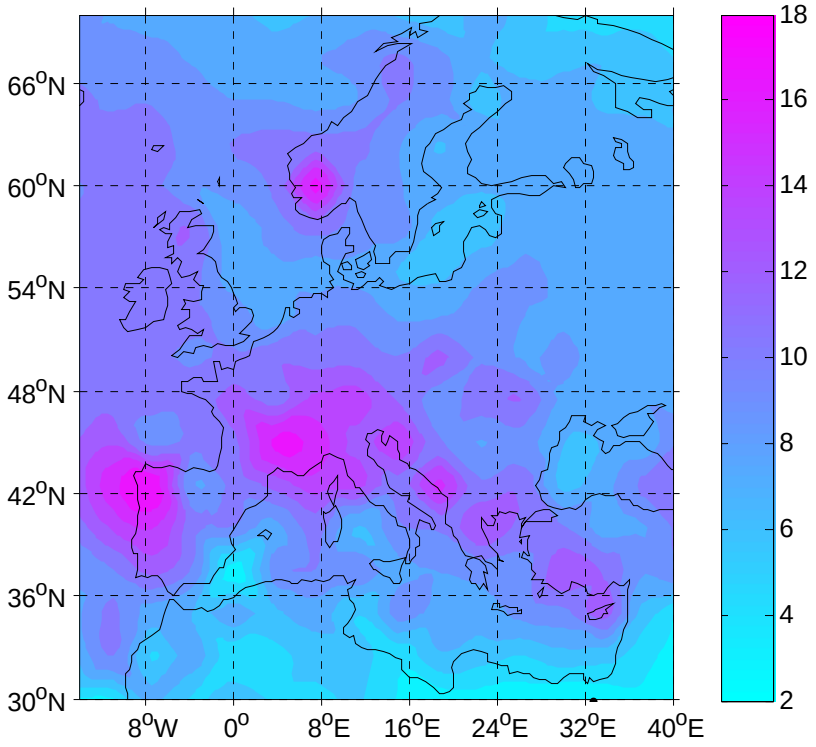

Figure 8 95th percentile (1961-90) of daily total rainfall (mm)

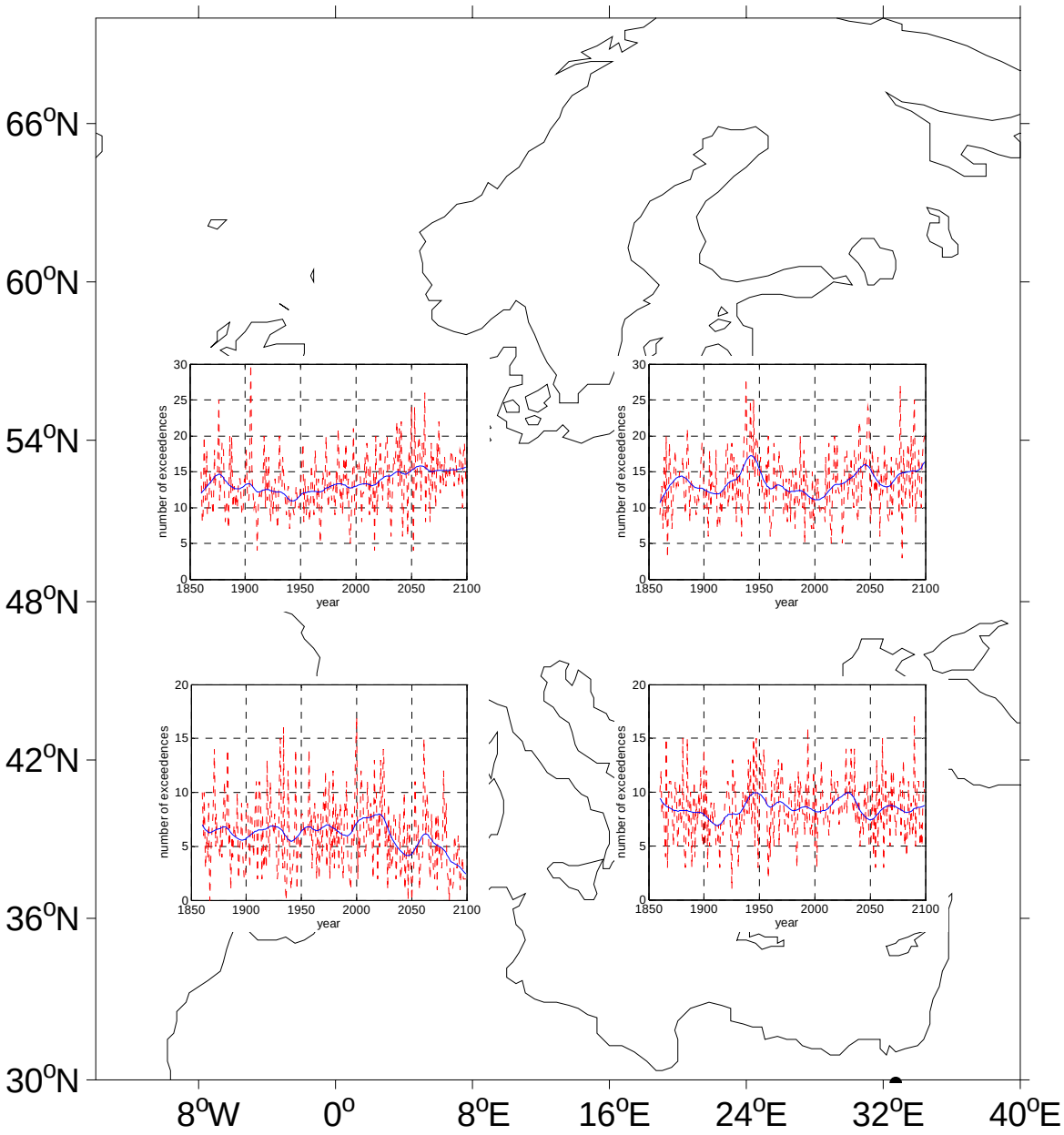

Figure 9 Exceedences of the 95th percentile (1961-90) of daily total rainfall

To further examine heavy rainfall events, Figure 10 shows time series of the annual maximum running total rainfall over 3 days. Apart from the UK, there is no change and, therefore, no health impact anywhere in Europe. The UK is projected to have a small increase in heavy rainfall from about 2060, but given the uncertainty in the model rainfall, it would be imprudent to attribute any health impact to this.

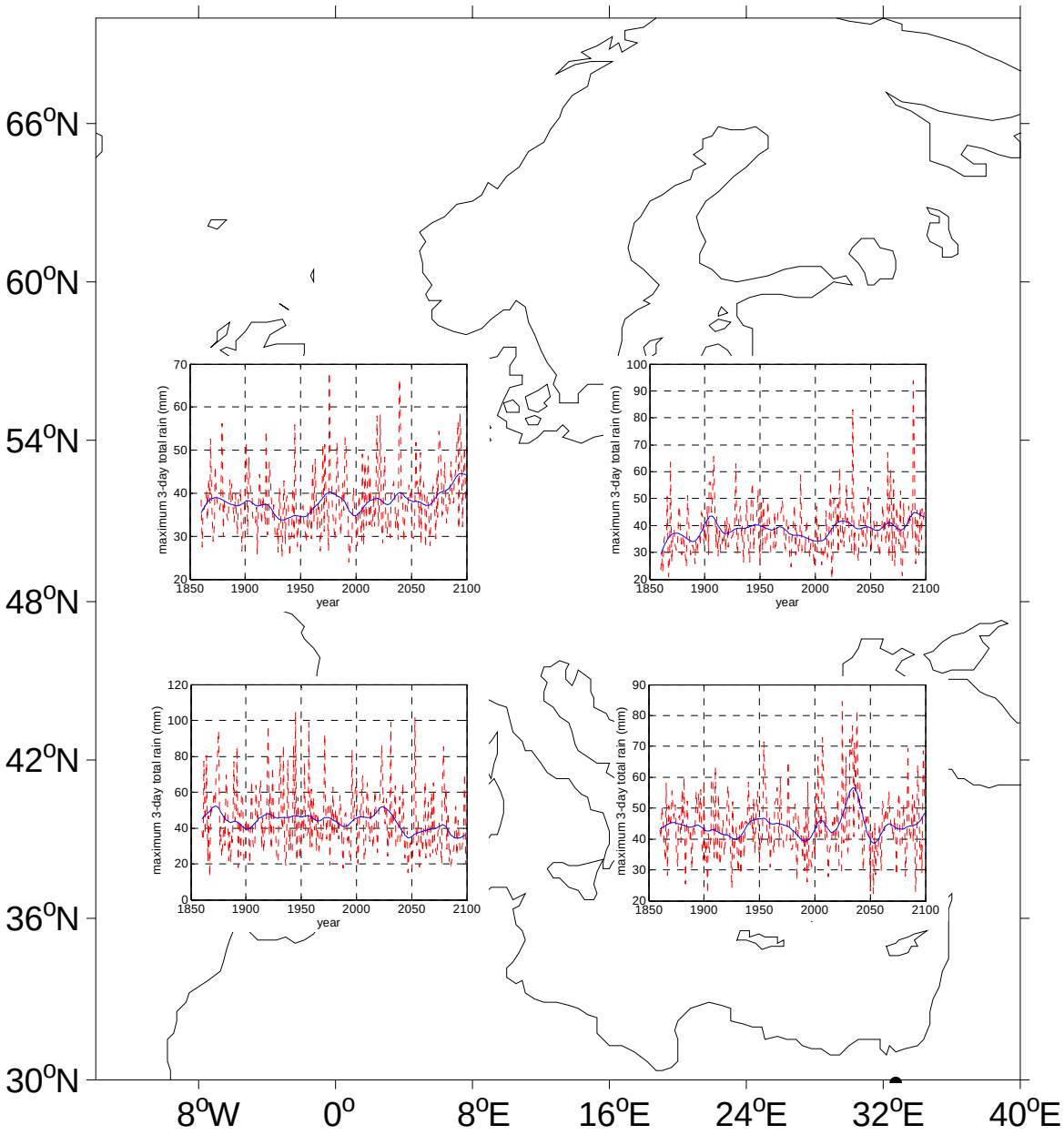

Figure 10 Annual maximum 3-day running total rainfall (mm)

To complete the examination of rainfall tendencies over Europe, Figure 11 shows time series of the annual maximum length of drought. This is determined as the longest spell in each year when rainfall did not exceed 0.1 mm on any day. Drought is projected to increase everywhere and, given the unprecedented changes, it is not possible to say what the health impacts might be. However, it is reasonable to speculate that stress-related health issues will arise, particularly in water-related industries such as agriculture. This discussion will be extended when the analysis is performed using the ENSEMBLES RCM data.

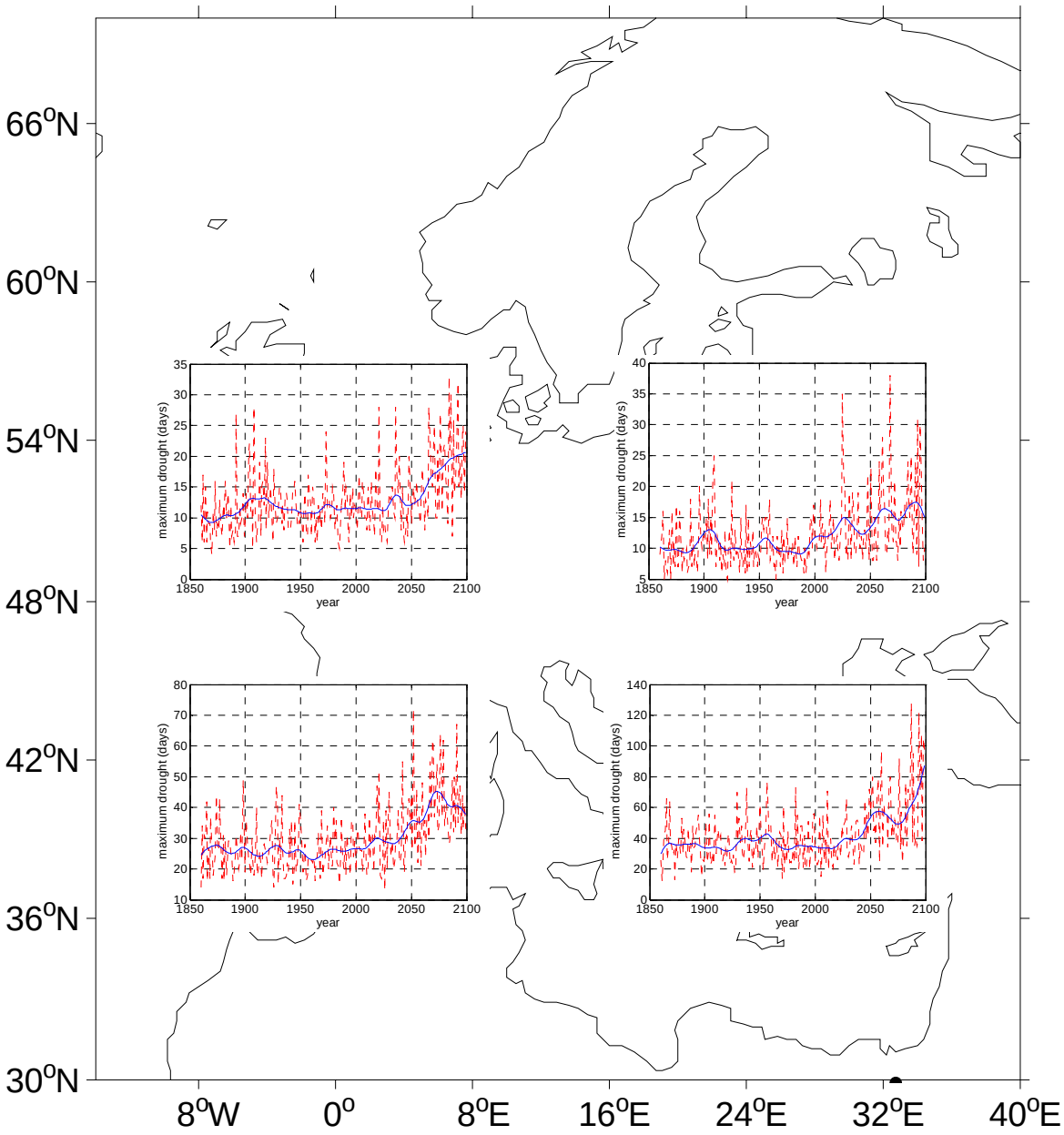

Figure 11 Annual maximum length of drought

Heat waves

The discussion on minimum mortality band established that, according to the model used here, cold-related mortality can be expected to decline over all of Europe as a result of global warming. At the same time, heat-related mortality is likely to increase. Here, we examine the issue of heat waves further.

The most recent and very severe European drought was the event in 2003. Although this affected mainly France causing many fatalities, it had an impact on neighbouring countries, including the UK. Examination of NCEP reanalysis data for UK during this drought revealed that for a grid point near Cambridge the 7-day running mean tmax was over 25°C for a total of six days. Comparison of NCEP with HadCM3 over the same grid point suggests that the model is about 2°C warmer than the reanalysis at that point. 27°C is roughly the 98th percentile (1961-90) of the HadCM3 data at the Cambridge grid point, giving us a yardstick to apply to all of Europe in terms of the 2003 heat wave. Counting the number of days per

year, at each grid point, where 7-day running mean tmax exceeds the 98th percentile (1961-90) yields time series from 1860-2099 comparing local conditions to what the local equivalent of the 2003 heat wave would have been.

Figure 12 shows that the local equivalent of heat waves such as the 2003 event will become relatively common over all of Europe from about 2050 onwards.

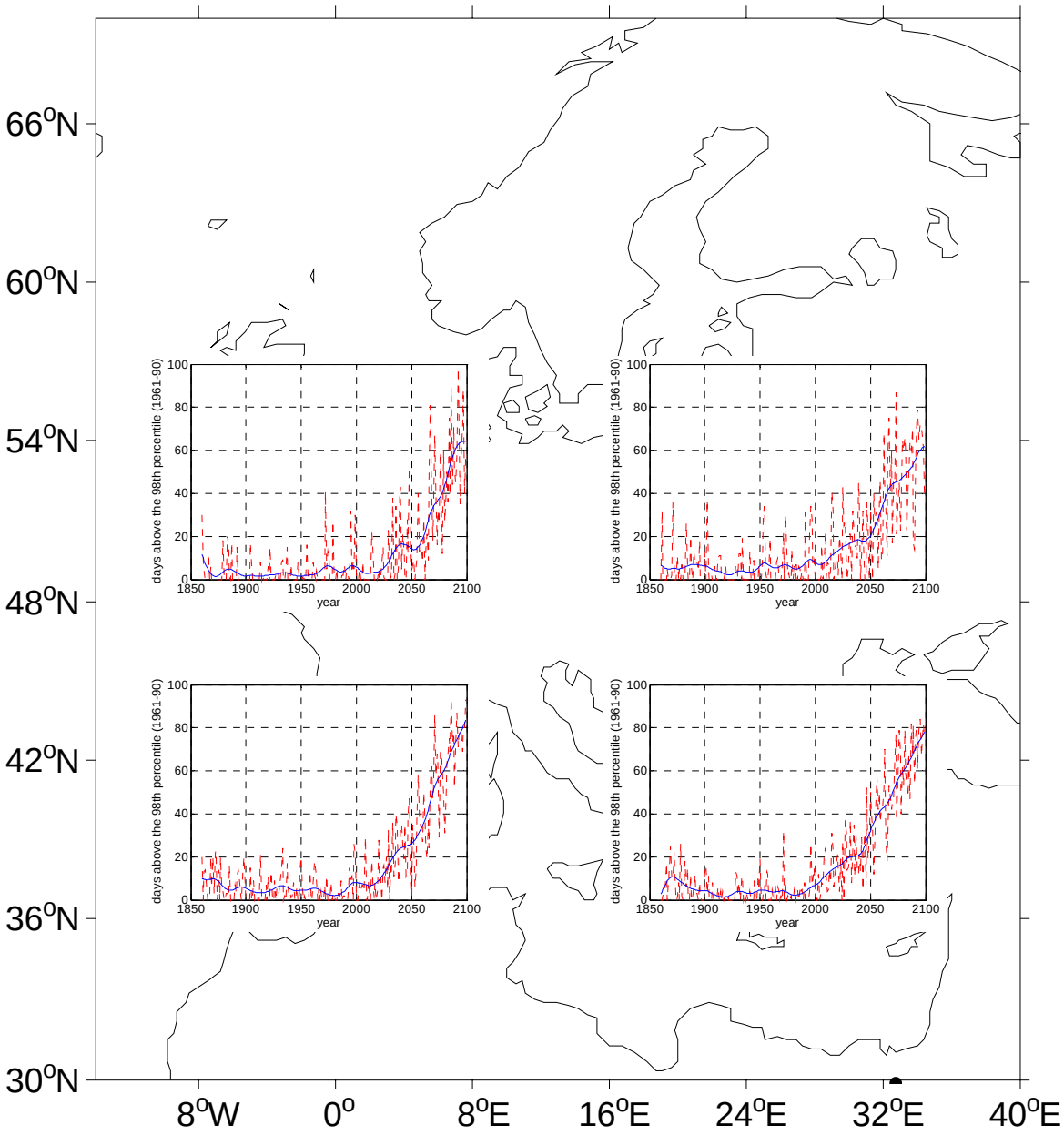

Figure 12 Number of days per year when 7-day running mean daily tmax exceeded the 1961-90 98th percentile

Summary

A series of statistical analogue models has been presented, relating climate change to health over the whole of Europe. Although the presentations are intended simply to demonstrate the models, and cannot be used to give definitive results without the ENSEMBLES RCM data, a number of general conclusions can be drawn:

- Cold-related health problems are likely to become less of a problem over all of Europe
- Heat-related problems will become more prevalent but are easier to deal with
- Injury and Stress issues related to inland flooding are unlikely to change, although the model used here does not give reliable estimates of intense rainfall.
- There will be little change in wind-related health issues.
- Winter pollution episodes are likely to become less frequent
- Summer pollution episodes will become more frequent if vehicle emissions control legislation is relaxed. Otherwise, emissions control will counter increased frequency of climate currently associated with summer pollution episodes.

Heat Stress

Several issues related to heat stress have been examined in the section on climate health impacts. However, heat stress also affects sectors such as agriculture, tourism, and energy. Figures 13 and 14 show the 95th percentile (1961-90) of July tmax, and exceedences of it, respectively. These figures give an overview of the distribution of high temperatures over Europe and how they are expected to change relative to current extremes. It is clear that temperatures currently regarded as unusual in early summer, will become the norm.

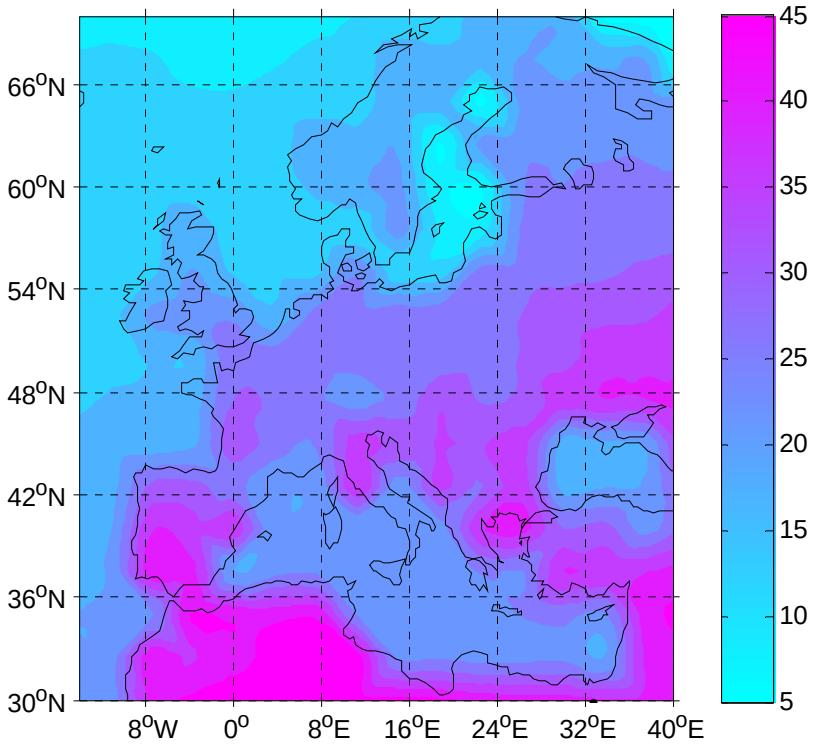

Figure 13 95th percentile (1961-90) of July tmax (°C)

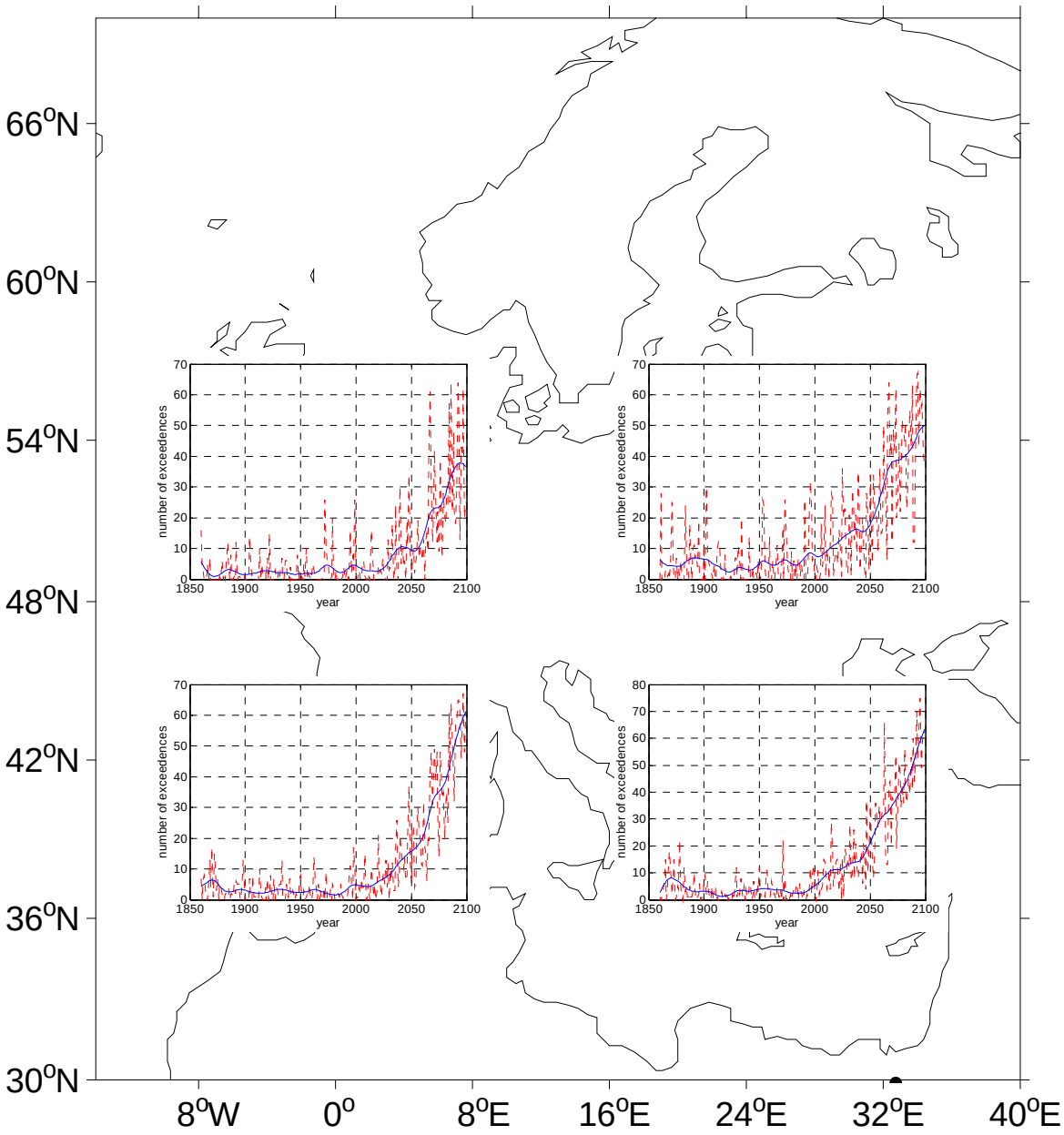

Figure 14 Exceedences of the 95th percentile (1961-90) of July tmax

Wind Storm

Indices have been produced relating wind speed from model data to the Beaufort scale. These include categories for gale, strong gale, storm, severe storm, and hurricane. A range of impacts is associated with each of these categories, allowing impact assessment of wind under climate change to be made. Unfortunately, as shown in the section on health, the ENSEMBLES RCM data are needed to examine these categories, GCM time series suffer from too much spatial smoothing to resolve these features of climate.

Return Levels

A return level is defined as the value of a variable which, on average, will be exceeded once every n years. Return levels are routinely used to describe changes in extremes and usefully combine information on the mean and variance of a sample of extremes in a single parameter. Since we are dealing with annual extremes, presumed to be iid (independent and identically-distributed) and to follow the Generalized Extreme Value (GEV) distribution, the mean and variance are calculated using the parameters of the GEV distribution and are expressed as $mean_{GEV}$ and $variance_{GEV}$. The GEV provides an appropriate model for block maxima (Coles, 2001), giving a good fit to empirical data that meet the iid criteria. Blocks of one year are commonly used since the interval is large enough to eliminate the issue of dependence between extremes and a common distribution for the individual extremes is a reasonable assumption. For a complete discussion of the theoretical basis of the GEV distribution see, for example, Coles (2001).

There are several ways to estimate the parameters of the GEV distribution (see Coles (2001) for a discussion). Here we use two of the most commonly-used methods, the maximum likelihood (ML) estimator and the probability weighted moments (PWM) estimator, in succession. The algorithms are slight modifications of the Matlab routines in the WAFO Toolbox (Brodtkorb et al, 2000). We first attempt to estimate the parameters using the ML method. This is our preferred estimator because the PWM method yields a wider range of parameter values with greater variance, and arguably less stable parameters. If the ML method has not provided stable parameters after 500 iterations, the PWM method is applied. If that fails, usually because the shape parameter exceeds acceptable limits, the empirical data is judged to have a distribution other than the GEV distribution (for succinctness, described as "not fitting the GEV model").

The GEV distribution is defined by its Cumulative Distribution Function (CDF) (Coles, 2001; Kotz and Nadarajah, 2000):

$$F(x;k,s,m0) = \exp\left\{-\left[1-k\left(\frac{x-m0}{s}\right)\right]^{\frac{1}{k}}\right\} \text{ if } k \cong 0 \quad OR$$

$$F(x;k,s,m0) = \exp\left\{-\exp\left[-\left(\frac{x-m0}{s}\right)\right]\right\} \text{ if } k = 0$$

where: x = a series of block maxima (such as annual extremes)

$m0 = location\ parameter$

$k = shape\ parameter$

$s = scale\ parameter$

N.B. $mean_{GEV}$ only exists if $k > -1$ and $variance_{GEV}$ only exists if $k > -0.5$ (Coles, 2001)

And the return level is calculated using:

$$z_p = \begin{cases} m0 - \frac{s}{k}\left[1 - \{-\log(1-p)\}^{-k}\right] & for \quad k \neq 0 \\ m0 - s\log\{-\log(1-p)\} & for \quad k = 0 \end{cases}$$

where: z_p is the return level associated with the return period $\frac{1}{p}$, and z_p is exceeded by the annual maximum in any particular year with probability *p*.

100-year return levels are the values which, on average, are expected to be exceeded once in a hundred years. The 100-year return period is chosen because it is commonly used in the literature when extrapolating from relatively short time series. Coles (2001) provides several examples and points out that such extrapolation is based on "unverifiable assumptions" and is critically dependent on the range of values of the GEV parameters.

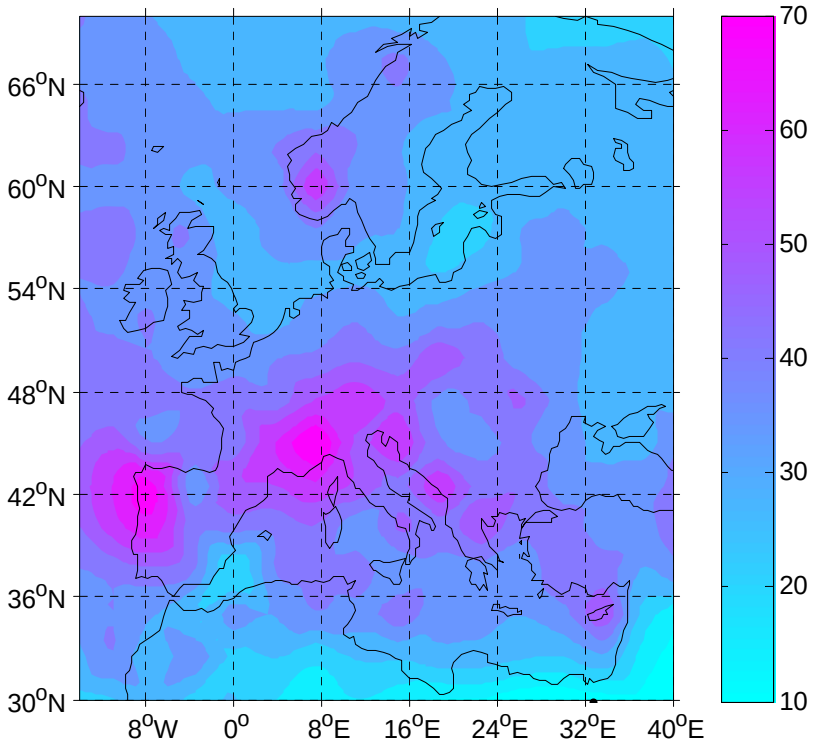

Figure 15 Annual maximum 3-day running total rainfall averaged 1961-90 (mm)

To illustrate the method, we will take the example of annual maximum 3-day running total rainfall for the period 1961-90. Figure 15 shows the average over this period. The 100-year return level calculated using the GEV is shown in Figure 16. The values shown in Figure 16 can be expressed as "the 1 in 100-year event". For example, one could say that, on average, one would expect the annual maximum 3-day running total rainfall over Portugal to exceed 180 mm once every 100 years. The method can be reversed, so that one could express an amount of rainfall and derive the return period, or interarrival time.

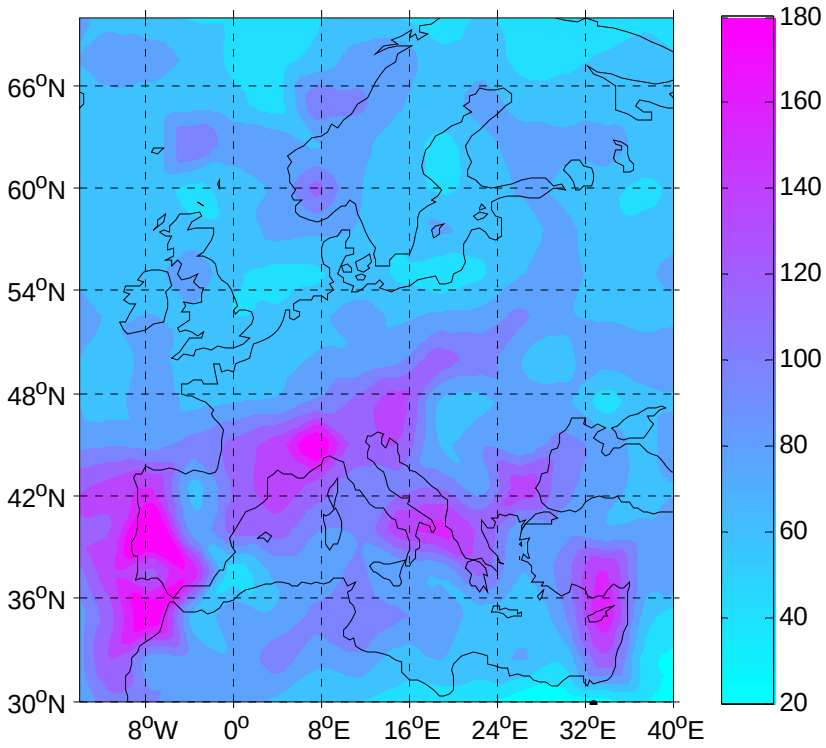

Figure 16 Annual maximum 3-day running total rainfall, 100-year return level (mm)

References

Brodtkorb, P.A., P. Johannesson, G. Lindgren, I. Rychlik, R. Ryden, and E. Sjö, 2000: WAFO – a Matlab toolbox for the analysis of random waves. Proceedings of the 10th ISOPE Conference.

Coles, S., 2001: An Introduction to Statistical Modeling of Extreme Values. Springer Series in Statistics, Springer-Verlag, London, ISBN 1-85233-459-2, 208 pp.

Kotz, S., and S. Nadarajah, 2000: Extreme Value Distributions: Theory and Applications. Imperial College Press, London, ISBN 1860942245, 185 pp.

Contribution to ENSEMBLES Deliverable D6.2

Report of 8 March 2006 from UREADMM

Tim Wheeler, Andrew Challinor, Tom Osborne, University of Reading, UREADMM

Impact Model Description: Crop productivity model

Name/acronym: GLAM (General Large Area Model for annual crops)

References:

Challinor, A.J., Wheeler, T.R., Craufurd, P.Q., Slingo, J.M., Grimes, D.I.F. (2004). Design and optimisation of a large-area process-based model for annual crops. Agricultural and Forest Meteorology 124: 99-120.

Challinor, A.J., Wheeler T.R., Craufurd P.Q., Slingo J.M. (2005). Simulation of the impact of high temperature stress on annual crop yields. Agricultural and Forest Meteorology, 135 (1-4): 180-189.

Introduction

There is increasing evidence from crop experiments that short-term climate events of only a few days duration can severely impact crop productivity if they coincide with a sensitive phase of crop growth. One example is the occurrence of high temperatures near to the time of crop flowering (Wheeler et al., 2000, Agriculture, Ecosystems and Environment 82: 159-167. Figure 1). It is now thought that how crops respond when these climate thresholds are exceeded will be a vital part of the impact of climate change on crop productivity in some regions. We have quantified the response of groundnut, wheat and rice crops to short-term high temperature events, and how this response differs among varieties of groundnut and rice, in controlled environment experiments. The modelling of the impacts of high temperature extremes can now be developed using these observations.

Figure 1. The effect of a 1 day high temperature event on the fruit / seed set of groundnut plants grown in controlled environments

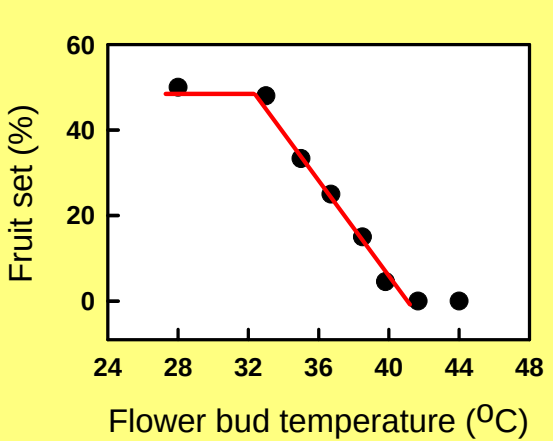

Model development for high temperature extremes

A full description of how the impact of high temperature extremes on groundnut crops are simulated in GLAM-HTS is given in Challinor et al. (2006). In brief, the first stage of the simulation of high temperature stress is the identification of episodes of high temperature. This is done by comparing the mean 8am to 2pm (solar time) temperature to a pre-defined critical value and to the development stage of the crop (pre- and post-anthesis). The critical temperature above which pod-set begins to be affected, and the temperature at zero pod-set, are defined and pod-set at intermediate temperatures is determined by linear interpolation. The reduction in the total pod-set is then given for each high temperature episode as a sum of the impact of that episode on each of the days during the flowering, where a flowering distribution prescribes the fraction of total flowers opening on each day. The fraction of yield-determining pods from the episode with the greatest impact is then used to modify the rate of change of harvest index, and hence crop yield.

Figure 2. Observed and simulated (a) yields and (b) pod-set as a fraction of the control (no high temperature) plants. The x-axis indicates the timing of the start of the six-day high temperature episode. Simulations using six flowering distributions are

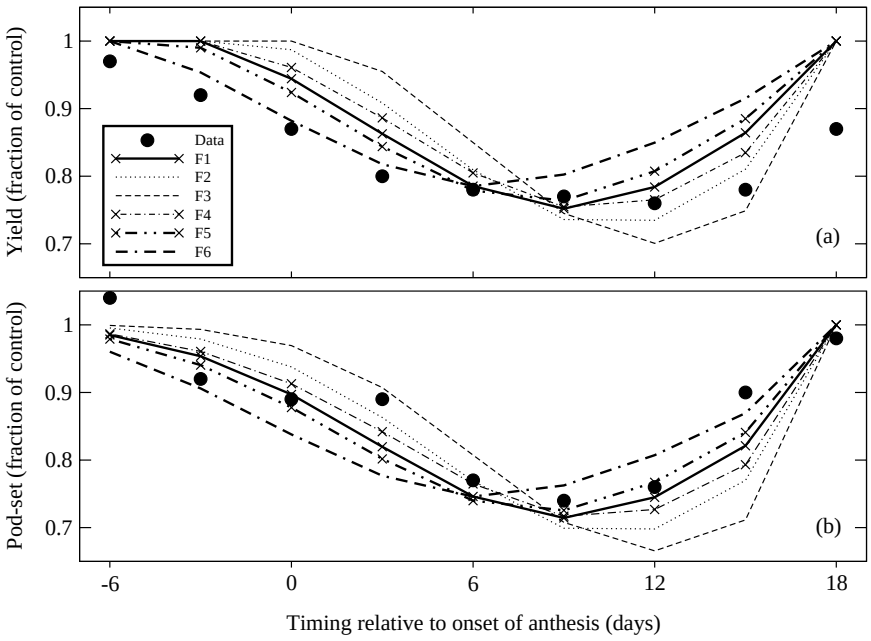

Comparison of model simulations with observations

Model simulations were compared with crop responses to high temperature episodes imposed using a range of controlled environment experiments (Challinor et al., 2006). For example, Prasad et al. (1999, Crop Science, 39, 1352-1357) reported a significant impact of high temperature on pod-set and pod weight of groundnut. These results are compared with GLAM-HTS run with a range of flowering distributions in Figure 2. The choice of flowering distribution in the model affected the simulations. The impact of the timing of the high temperature episode relative to anthesis on pod-set and yield was captured by the model. Most of the absolute difference between simulated and observed yields were less than 10% of the control yield.

Skilful simulation of the effects of short-term temperature extremes also relies on good prediction by the crop model of the effects of mean temperature on the rate of crop development. For example, good simulations of the impacts of temperature extremes at sensitive stages of a crop will be of limited value for prediction if the timing of crop development is not also well simulated. Figure 3 shows the simulated and observed impact of seasonal mean temperature on groundnut crop duration. GLAM-HTS was capable of reproducing the observed impacts of mean temperature on crop duration. The mean simulated duration (across the three simulations) is within 5% of observed values at all three temperatures. The mean simulated change in duration from 20°C to either 24 or 28°C is within 8% of the observed mean change (that is, 5 days).

Figure 3. The simulated and observed impact of seasonal mean temperature on total crop duration. Observations are from Nigam *et al.* (1994, Annals Applied Biology,

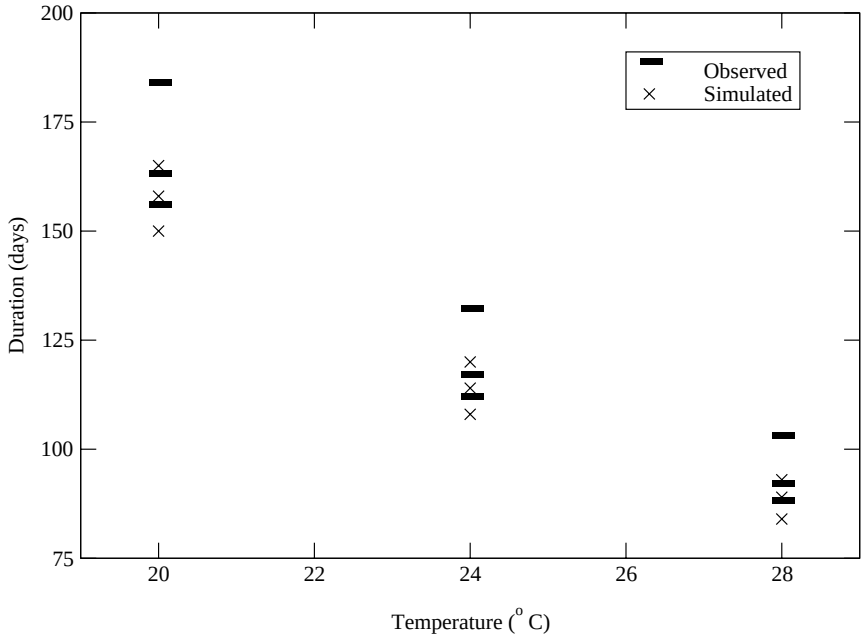

Conclusion

Crop response to high temperature extremes has now been incorporated into GLAM to give us a GLAM-HTS (high temperature stress) model version. This opens up opportunities for us to examine how short-term, inter-seasonal variability in temperature will affect crop productivity in current and future climates.

Contribution to ENSEMBLES Deliverable D6.2

Report from NOA: A Heat Index for heat stress studies

Christos Giannakopoulus, Effie Kostopoulou: National Observatory of Athens

The Heat index (HI) is an index that combines air temperature and relative humidity to determine an apparent temperature — how hot it actually feels. The human body normally cools itself by perspiration, or sweating, in which the water in the sweat evaporates and carries heat away from the body. However, when the relative humidity is high, the evaporation rate of water is reduced. This means heat is removed from the body at a lower rate, causing it to retain more heat than it would in dry air. Measurements have been taken based on subjective descriptions of how hot subjects feel for a given temperature and humidity, allowing an index to be made which corresponds a temperature and humidity combination to a higher temperature in dry air.

At high temperatures, the level of relative humidity needed to make the Heat Index higher than the actual temperature is lower than at cooler temperatures. For example, at 27 °C, the heat index will agree with the actual temperature if the relative humidity is 45%, but at 43 °C, any relative humidity reading above 17% will make the Heat Index higher than 43 °C. Humidity is deemed not to raise the apparent temperature at all if the actual temperature is below approximately 20 °C — essentially the same temperature colder than which wind chill is thought to commence. It should be noted that heat indexes are based on temperature measurements taken in the shade and not the sun, so extra care must be taken while in the sun.

Formula

The formula for calculating the heat index using the air temperature in degrees Celsius and the relative humidity is:

$$HI = T + \frac{5}{9}(e - 10)$$

where,

$$e = V(6.112x10^{\frac{7.5T}{(237.7+T)}}\frac{R}{100})$$

and

V = Vapour pressure
R = Relative humidity (%)
T = Temperature (°C)

Effects of the heat index (shade values)

Celsius	Notes
27–32 °C	Caution — fatigue is possible with prolonged exposure and activity
32–41 °C	Extreme caution — sunstroke, heat cramps, and heat exhaustion are possible

41–54 °C	Danger — sunstroke, heat cramps, and heat exhaustion are likely; heat stroke is possible
over 54 °C	Extreme danger — heat stroke or sunstroke are likely with continued exposure

Note that exposure to full sunshine can increase heat index values by up to 15 °F (8 °C).

Data and heat stress results for Athens

Meteorological data from the station of the National Observatory of Athens at the centre of Athens were used for the period 1993-2001. This period coincides with the period that hospital admissions data were made available to us, so in the future it will be possible to examine synergistic effects of heat stress with hospital admissions.

In the graphs that follow we have calculated the cumulative amount of days (for the above mentioned period) that the heat index falls in the categories outlined in the above table (no caution, caution, extreme caution). No danger/extreme danger class categories were found for Athens at least for shade conditions.

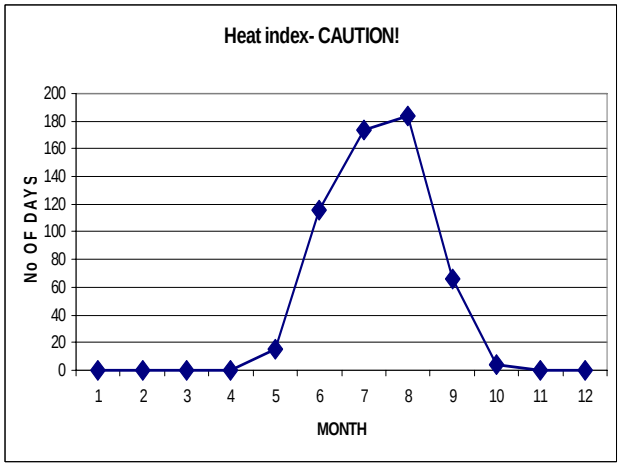

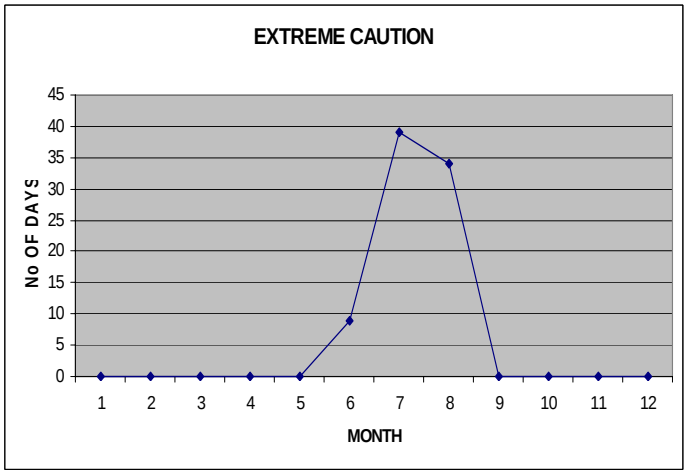

Contribution to ENSEMBLES Deliverable D6.2

Report from FUB: A Storm Damage Regression Model (SDRM)

Uwe Ulbrich, Gregor Leckebusch: Free University of Berlin

Introduction

The Storm Damage Regression Model (SDRM) estimates loss values for property damage caused by extreme wind speeds. Linear regression is used to link observed property damage to wind values above a specific thresholds.

The required input climatic variable is daily maximum wind speed at 10 m. This is used to give annual maxima, currently on a 1°x1° latitude/longitude grid. The spatial grid resolution depends on the available input data.

Phases of model implementation

1. Calculation of normalized cubic wind from input data. Where input data can be from reanalysis (e.g. NCEP, ERA-40), global Earth System Models (ESMs), or Regional Climate Models (RCMs).
2. GIS analysis and visualisation (ArcView/ArcGIS)
   including global population distribution data on 1x1 degree grid
   including calculation of damage potential per grid box
3. Calculation of accumulated damage potential for different time slices and/or regions
4. Fitting the calculated damage potential per year and region to observed losses, using linear regression.

Current status of the model

The model will be applied to ENSEMBLES ESM and RCM output, when available, using the multi-scenarios approach. The model has been calibrated and tested in ENSEMBLES using data from the UK Met Office Hadley Centre models, HadCM3 and HadRM3P.

References

Klawa and Ulbrich, 2003: A model for the estimation of storm losses and the identification of severe winter storms in Germany. Natural Hazards and Earth System Sciences, Vol. 3, 725-732